Risk-targeted Maps for Spain

Alireza Kharazian (alireza.kharazian@ua.es)
University of Alicante: Universitat d'Alacant
Sergio Molina
University of Alicante: Universitat d'Alacant
Juan Jose Galiana-Merino
University of Alicante: Universitat d'Alacant
Noelia Agea-Medina
University of Alicante: Universitat d'Alacant

Research Article

Keywords: seismic hazard, earthquake engineering, collapse probability, risk targeting, fragility models

Posted Date: February 17th, 2021

DOI: https://doi.org/10.21203/rs.3.rs-226357/v1

Version of Record: A version of this preprint was published at Bulletin of Earthquake Engineering on July 29th, 2021. See the published version at https://doi.org/10.1007/s10518-021-01189-8.

Abstract

Many studies have demonstrated that the design of structures in the region through the *uniform hazard* principle does not guarantee the uniform collapse risk. Even in those regions with similar PGAs corresponding to the same mean return period, the seismic risk in terms of failure probability will be significantly different due to the structural capacity uncertainty. In this paper, the newly introduced method, known as *risk targeting*, is being explored in Spain using the recently updated seismic hazard map. Since risk targeting involves multiple input parameters such as model parameters of fragility curves, their variability is considered through their probability distribution corresponding to the RC moment frame building, which is the most common typology in Spain. The influence of variation of these parameters on the risk results are investigated and different assumptions for estimating the model parameters of fragility curves are illustrated. These assumptions are included in a fixed fragility curve (generic) or building-site-specific fragility curves. Different acceptable risk levels (i.e., collapse and yielding) were considered concerning the Spain seismicity level. Finally, the maps for risk-targeted design ground motion and risk coefficient are presented. It was outlined since the shape of the hazard curve across Spain is different and considering the uncertainty of structural capacity; the employment of risk-targeted analysis led to the modifications for existing design ground motions. Moreover, it was found that using the building- and site-specific fragility curves could provide better results.

1 Introduction

Seismic assessment and structural design are continually evolving, as evidenced by the rapid development of new procedures illustrated by the Pacific Earthquake Engineering Research Center (PEER). Numerous studies aimed to integrate the principle of probability into seismic performance evaluation, taking into account the uncertainties related to seismic input and structural properties, capacity, and model (Dolšek 2009; Liel et al. 2009). To estimate the seismic demand at a specific location, the vast majority of the Earthquake Design Codes rely on a seismically defined return period (for example, 10% in 50 years) of intensity measures. The decision to design the structure following a *uniform hazard* level is based on the idea that a process like this leads to the same annual probability of collapse anywhere in the buildings. Nevertheless, this happens only if the collapse probability is a certain value which is infeasible in real cases. Multiple studies have recently demonstrated that a design-based earthquake determined on a uniform hazard theory does not necessarily lead to the design of structures with a consistent risk of collapse in different areas. These inconsistencies are due to the different shapes of the hazard curve for different regions and uncertainties in the failure capacity of structures (Luco et al. 2007) arising from a set of factors, such as different material properties, differences in design, and among others. This uncertainty also can be raised from the record-to-record variability corresponding to the demand (e.g., uncertainty in ground motion). Hence, a structure can collapse for a different ground motion from what it was designed for. Moreover, as the shape of the hazard curve depends on the site location, even the buildings designed for the same ground motion will have different collapse probability values.

Based on the work done by Luco et al. (2007), the estimation of a design ground motion to provide a constant level of risk would be more consistent with using *uniform risk* assumption. This algorithm was used to present the risk-targeted maximum considered earthquake (MCE) ground motion (ASCE 2016). Accordingly, using the proposed method, Douglas et al. (2013) presented a risk-targeted seismic design map for France. In the study performed by Silva et al. (2016), various parameters involved in developing risk-targeted design maps are analyzed, and maps for Europe created using SHARE seismic hazard results (www.share-eu.org). The risk-targeted map of Romania was developed by Vacareanu et al. (2018), using the hazard models developed by Pavel et al. (2016). Spillatura et al. (2018) applied site- and structure-specific fragility curves to estimate the risk-targeted design ground motion. Iervolino et al. (2018) addressed some research results relating to the risk of failure in residential and industrial construction compliance with the Italian code. They showed that seismic structural reliability tends to decrease with increasing seismic hazard to the building site, despite the homogeneous return period of excess seismic design ground motion. Douglas and Gkimprixis (2018) presented a review of the state of the art of this technique, highlighting efforts to constrain better some of the input parameters. Besides, they discussed the problems in the practical implementation of this approach and the alternative forward paths. Zaman and Ghayamghamian (2019) performed the probabilistic seismic hazard analysis, and a risk-targeted map for Tehran was provided based on the hazard curves achieved. Taherian and Kalantari (2019) presented a risk-targeted seismic design map for Iran, considering the seismic hazard models from different seismic hazard maps. In recent work, Taherian and Kalantari (2021) performed a risk targeting analysis for a case study of Iran for two hazard levels, i.e., design ground motions with mean return periods of 475 and 2475 years. To evaluate alternative approaches, Gkimprixis et al. (2019) performed a review and comparison among the existing procedures concerning the implementation of uniform-risk concepts in the performance-based design of structures. Among these, one based on the use of risk-targeted behavior factors (RTBFs) has been recently considered to develop future versions of Eurocode 8 (EN-1998 2005). Douglas et al. (2019) demonstrated the effects of the RTBF approach being applied to the concept of risk-targeted maps for Italy.

While some research has been carried out on the importance and influence of input parameters in risk analysis, only a few studies, e.g., Martins et al. (2018), have attempted to consider the distribution of these parameters considering their variability through this probability framework in risk targeting analysis. This paper tries to develop new risk-targeted seismic design maps for Spain contemplating two different risk levels, i.e., collapse and slight damage state. This research aims to determine whether there would be a significant variation in the current design PGA values while considering the uniform risk assumption. In this study, using the updated seismic hazard in Spain (Benito et al. 2013) and the employment of variability in model parameters of fragility curves, the risk-targeted ground motion distribution is estimated for the region. It should be noted that these maps are obtained for the design of new structures using seismic design codes such as Eurocode 8. Moreover, we assumed the most common buildings in Spain are RC moment frame buildings.

2. Seismic Hazard Model

Spain is a country of moderate to low seismic hazard when compared with other European countries as Italy or Greece. However, the country has suffered several damaging earthquakes being the most important: the 1829 Torrevieja earthquake with a maximum intensity IX-X and Mw 6.6 and the 1884 Arenas del Rey earthquake with a maximum intensity IX-X and Mw 6.5 (Mezcua et al. 2004). Therefore, the first national seismic code using a probabilistic seismic hazard map was approved in 1994. The seismic code was updated with a new map in 2002 and recently after the damaging earthquakes that occurred in the southeast of Spain (1999 Mula earthquake, 2002 Bullas earthquake, 2005 La Paca earthquake, and 2011 Lorca earthquake with moment magnitudes between 4.7 and 5.2), the seismic hazard map was again updated to be used in the next Spanish seismic code.

The new seismic hazard map (IGN-UPM Working Group 2013) was the result of a project carried out by the National Geographic Institute (IGN) and the Earthquake Engineering Research Group of the Technical University of Madrid (UPM). Here, we used the seismic zoning provided by ZESIS (Garcia-Mayordomo 2015; IGME 2015) and the activity rate, b-parameters, maximum magnitude, and ground motion prediction equations suggested by (IGN-UPM Working Group, 2013) to compute the seismic hazard map for the Iberian Peninsula in a grid of 0.1 x 0.1 degrees using the software R-CRISIS (Ordaz et al. 2013). The whole grid has 150 x 90 points, where the PSHA has been obtained in terms of PGA at rock (Fig. 1).

Therefore, a total of 13500 sites were taken from PSHA results for the selected area. Figure 2 represents the seismic hazard curves of PGA in terms of annual probability of exceedance for some of the cities with the highest seismic hazard, i.e., Valencia, Alicante, Murcia, Almeria, Granada, and Malaga (Fig. 1).

From Fig. 2, we can see that the two cities of Valencia and Malaga have almost the same ground motion corresponding to the mean return period (RP) of 475 years (i.e., PGA = 0.147g and 0.152g, respectively). However, as noted, the disparity in the form of the hazard curve (Fig. 2) contributes to unequal values of the failure probability (P_c) in 50 years (see the following section), e.g., $P_c = 2\times10^{-3}$ and $P_c = 1.4\times10^{-3}$ for Valencia and Malaga, respectively. It confirms that the buildings designed for the same ground motion could have different values of failure probability. However, if we estimate the distribution of local hazard curve slopes for seismic actions between 2475 and 475 years (Jalayer and Cornell 2003) for each site in Spain (Fig. 3), we confirm that at the national level, not much variation can be expected in risk-targeted design ground motions due to the almost similar slope of hazard curves. Nevertheless, the risk-targeted design ground motions depend not only on the shape of the hazard curve but also on the input parameters of the related fragility curve and the acceptable risk level (see following sections).

3 Computing Risk-targeted Ground Motions

In order to perform a risk-targeted analysis, it is necessary to develop the fragility curve corresponding to the structures under study. Considering that in this approach, the fragility curves should cover the vulnerability of an extensive range of different building typologies and on the other hand, developing these curves are too expensive for a specific building class and location, the generic collapse fragility curves will be used for all building classes. It should be noted that the provided curves must be

sufficiently generic to capture all possible vulnerabilities (Douglas et al. 2013). The fragility function is conditional upon the values of design ground motion. It outlines the conditional probability of exceeding or reaching a limit state, which from now on is the collapse of a structure or the slight damage (yielding), for a given design ground motion with a specific RP. In this study, the 475- and 95-year RP are implemented (i.e., 10% probability of exceedance in 50 years and 10% probability of exceedance in 10 years). These RPs are reference seismic actions in EC8, contributing to the criteria for no-collapse and damage limitation requirements. The fragility functions are presented as lognormal distributions with two parameters: the median value of desired intensity measure, e.g., PGA with 50th-percentile of a probability distribution, and the logarithmic standard deviation of PGA (β). Hence, to develop a generic fragility curve for risk-targeted analysis, it is needed to define the parameters of $P_{ds}|gm$ (let say any percentile value of probability distribution related to a damaged state), and β. The subscript *ds* represents the damage state: *c* collapse and *y* slight so throughout this paper, the term "$P_{ds}|gm$" will refer to the conditional probability of collapse ($P_c|gm$) and to the probability of exceeding a slight damage state or yielding ($P_y|gm$) at design ground motion. The former parameter (β) takes into account several causes of capacity uncertainty, such as record-to-record variation, uncertainty in the definition of damage state, and ideally other causes such as human errors, which cannot be supported by the most advanced numerical models (Silva et al. 2016).

It should be outlined there is no guidance regarding the fragility curves of structures designed based on the EC8 in this building code. Thus far, previous studies have suggested different values for the parameter of β. As an example, Luco et al. (2007) used a β value of 0.8, while Douglas et al. (2013) suggested a value of 0.5. A β value of 0.6 was considered in the study by Silva et al. (2016), while Vanzi et al. (2015) used a value of 0.2. It is important to note that using the higher values of β (i.e., more than 0.8) provides a low probability of collapse even in highly seismic regions, which seems an unrealistic scenario. On the other hand, assuming low values of β (e.g., less than 0.2) leads to more steep collapse fragility curves that could provide 100% probability of collapse even at low ground motion levels.

The estimation of $P_{ds}|gm$, needs the design and evaluation of many structures and a wide range of hazard levels. Several studies have postulated different values of $P_{ds}|gm$ either for collapse or yielding damage state. For instance, Douglas et al. (2013) suggested a $P_c|gm$ value of 10^{-5}, while Silva et al. (2016) used a value of 10^{-3}. Ulrich et al. (2014) demonstrated that for a design ground motion between 0.07g and 0.3g, the probability of yielding ($P_y|gm$) varies from 0.14 to 0.85, respectively. Moreover, they proposed a value for $P_c|gm$ with an order of 10^{-7} for low, frequent design ground motion levels and 10^{-5} for higher and rarer design ground motion in their study. However, Silva et al. (2016) believe this range of probability of collapse (i.e., 10^{-7} to 10^{-5}) is too extremely low for ordinary structures. Luco et al. (2007) selected 10% probability of collapse under MCE, which corresponds to the probability of collapse at 475-year ground motion ranging from 10^{-2} to 10^{-3}. Fajfar and Dolšek (2012) computed the value of $P_c|gm$ in the range of 10^{-4} to $10^{-5,}$ and Vanzi et al. (2015) used the value of 1.3×10^{-6} for the probability of

collapse under gravity loads. Taherian and Kalantari (2019) defined the $P_c|gm = 0.01$ and $\beta = 0.8$ for the Iranian code-conforming buildings.

According to the method proposed by (Luco et al. 2007; Kennedy 2011; Douglas et al. 2013) and using the given seismic hazard curve (Mean Annual Frequency, MAF, of exceeding various values of PGA) and failure fragility function (expressed as a probability density function, PDF) the annual failure rate of a structure (MAF of exceeding the damage state (ds)), is determined using the following classic convolution products given by Kennedy (2011):

$$MAF = \int_0^{+\infty} G(s).\frac{dF(s)}{ds}ds \qquad (1)$$

Where *F*(s) is the fragility function (conditional probability of collapse for a given ground motion), and *G*(s) is the hazard curve. The integration in Eq. (1) does not have a closed-form solution (Eads et al. 2013); therefore, an iterative process is required to calculate risk-targeted design ground motions. As suggested by (Eads et al. 2013; Silva et al. 2016), the annual failure probability will be computed by dividing both the fragility and seismic hazard curves into a large number of segments and then by numerically integrating the distribution. It should be mentioned that since we are targeting the minimal values and considering the Poisson assumption, there is a negligible difference between the annual probability of failure P_f and the annual failure rate (i.e., mean annual frequency of failure, MAF). The main objective is to estimate ground motion consistent with the target risk (i.e., the accepted annual failure rate). Therefore, it is necessary to define an acceptable level of seismic risk, expressed as annual collapse probability or annual probability of exceeding the yielding depending on the desired risk performance. Regarding with acceptable annual probability of collapse, there are different suggestions from other studies and seismic codes. For example, the American Society of Civil Engineers (ASCE 2016) proposed a value of 2.0×10^{-4} for the United States. This value is also considered by Luco et al. (2007). Douglas et al. (2013) suggested using 1.0×10^{-5} as a reasonable value. In the research carried out by Silva et al. (2016), the value of 5.0×10^{-5} was established as an acceptable annual probability of collapse. Taherian and Kalantari (2019) proposed the target annual collapse probability of 1% in 50 years.

Nevertheless, this threshold (i.e., the acceptable annual probability of collapse) depends on the importance of the structures (Douglas et al. 2013). It should be estimated by the policymakers, sociologists, and other related decision-makers, with engineers' aid. Also, regarding the design of new structures, Douglas et al. (2013), Silva et al. (2016), and Martins et al. (2018) suggested that the potential losses due to the more frequent earthquakes should be considered. For example, in Eurocode 8, the damage limitation has been introduced for ground motions with 10% probability of exceedance in 10 years (95-year return period). However, keeping in mind this cannot lead to a uniform risk across the area

or the structures. Hence it is recommended to develop risk-targeted hazard maps for a different level of risk, e.g., yielding or collapse limit states.

Therefore, in the iterative process, the value of design ground motion changes in each step until reaching the expected value of acceptable annual failure probability. The obtained design ground motion at the final step will be the risk-targeted ground motion. Based on the study by Luco et al. (2007), for each seismic site, the risk coefficient (CR) is calculated by dividing the obtained former value and the uniform hazard design ground motion with a specific mean return period.

4 Estimation Of Input Parameters For Spain (Pc|gm, β, And Acceptable Collapse Rate)

The estimation of $P_c|gm$ was the object of restricted studies since it involves assessing a wide variety of structures and analyzing a diverse range of hazard thresholds. The determination of the content of $P_c|gm$ from a comprehensive review of the fragility models existing in the literature is impractical because the modeling process and related design ground motions are not commonly recorded. Moreover, in the documentation related to the Spain seismic regulations, there is almost no guidance on what value to choose for the level of acceptable risk or conditional probability of collapse for a given design PGA and β.

In most recent studies such as Gkimprixis, Tubaldi, and Douglas (2020) and Crowley, Silva, and Martins (2018), the building-specific fragility functions have been implemented in risk-targeting analysis to avoid gaining overestimated values of collapse risk specifically for low hazard regions. Considering the variability of $P_c|gm$, and β in risk-targeted analysis, we decided to develop random variables distribution functions. The normal distribution of $P_c|gm$, and β are prepared according to the results obtained by Martins et al. (2018). They developed a set of regular RC moment frame structures designed with the most up-to-date European codes for different ground motion levels. Each structure was represented using a tri-dimensional finite element model and tested against a set of ground motion records using nonlinear dynamic analyses. They considered two damage states: yielding (onset of structural damage) and structural collapse. Variability in the structural design has been introduced to propagate the building-to-building variability to the risk estimates. Hence, in this study, we consider the RC moment frame buildings as a common typology in Spain.

Consequently, based on the previous assumptions and the results obtained by Martins et al. (2018), and considering the simultaneous effect of two parameters on the fragility curve, a multivariant probability distribution is developed, which is displayed in Fig. 4a. This distribution can capture the uncertainty in the parameters mentioned above in risk-targeting analysis. It should be outlined that Martins et al. (2018) and Silva et al. (2016) recommended considering the correlation between $P_c|gm$, and β to avoid developing unrealistic fragility curves. For instance, the higher values of β in high seismic hazard zones lead to the flatter fragility curve and, consequently, the low probability of collapse even for a higher ground motions level. Therefore, for developing the multivariant probability distribution shown in Fig. 4a, the correlation between $P_c|gm$, and β has been considered.

This multivariant probability distribution was employed to generate one hundred random fragility curves corresponding to different random values of $P_c|gm$, and β. Moreover, when sampling the parameters, the correlation between $P_c|gm$, and β has also been considered. Following considering the mean fragility curve (Fig. 4b), we calculated another time the annual rate of collapse across Spain once for all 100 developed $P_c|gm$, and β and then by repeating the same process but using the fragility function developed by Crowley, Silva, and Martins (2018), according to the methodology described in the preceding section. The obtained results were used for estimating the acceptable annual rate of collapse (see subsequent paragraphs).

Regarding with acceptable annual probability of collapse, there are different suggestions from other studies and seismic codes as discussed in Sect. 3. Herein, we performed a similar analysis to what Luco et al. (2007) have done to estimate the acceptable annual probability of collapse. To begin this process, the target probability of collapse is estimated through three different assumptions. In the first method, the fixed values of 0.7 and 3×10^{-4} were assumed for β and $P_c|gm$, respectively. These values were calculated by getting an average over all the sampled β and $P_c|gm$. The annual probability of collapse for all 13500 sites was then calculated. Table 1 presents the statistical results of collapse probability across the country, considering the assumptions mentioned earlier.

Table 1
Statistical results obtained from the risk analysis for Spain Pc|gm = 3×10− 4 and = 0.7 (mean fragility curve)

β					
	Max	**Min**	**Median**	**Mean**	**CoV***
Annual collapse rate	1.7×10^{-5}	2.9×10^{-7}	6.4×10^{-6}	7.0×10^{-6}	0.57
Probability of collapse in 50 years	8.3×10^{-4}	1.4×10^{-5}	3.2×10^{-4}	3.3×10^{-4}	0.58
*CoV: Coefficient of Variation					

Table 1 shows that the average annual probability of collapse is $7.0\times10^{-6,}$ and the maximum and minimum values are 1.7×10^{-5} and 2.9×10^{-7}, respectively. Therefore, it can be observed that in many areas, the values of the annual probability of collapse are different with respect to the average value of the risk rate (7.0×10^{-6}). Hence, the need for the development of risk-targeted seismic design maps for the country is obvious.

Once again, in order to consider all uncertainties due to the variability of building-to-building, all the possible values of β and $P_c|gm$ (100 random values of β and $P_c|gm$) are extracted from the multivariant normal distribution. The annual probabilities of collapse across Spain were calculated. The obtained results are summarized in Table 2.

Table 2
Statistical results obtained from the risk analysis for Spain (considering 100 random values of and Pc|gm using the normal joint distribution for each site)

	Max	Min	Median	Mean	CoV*
Annual collapse rate	3.1×10^{-5}	1.0×10^{-6}	1.0×10^{-5}	1.1×10^{-5}	0.64
Probability of collapse in 50 years	1.57×10^{-3}	3.7×10^{-5}	5.2×10^{-4}	5.7×10^{-4}	0.61
*CoV: Coefficient of Variation					

Table 2 shows that the average annual probability of collapse is $1.1\times10^{-5,}$ and the maximum and minimum values are 3.1×10^{-5} and 10^{-6}, respectively. The mean value in Table 2 has the same order of magnitude as the value proposed by Douglas et al. (2013) (order of 10^{-5}). Table 2 also shows the effect of variability of β and $P_c|gm$ on the annual probability of collapse and the importance of considering this variability in the probabilistic framework.

In the third option, for every 13500 sites, the corresponding values of β and $P_c|gm$ were estimated according to the fragility curve matching the design ground motion at the site. These values are calculated through the results obtained by Martins et al. (2018) and Crowley, Silva, and Martins (2018). They established a relationship between the design ground motion and the median and logarithmic standard deviation of the collapse fragility functions. Then again, through the same procedure as the previous two methods, the minimum, maximum, median, mean value, and coefficient of variation of the annual collapse rate are determined. Table 3 shows the statistical results.

Table 3
Statistical results obtained from the risk analysis for Spain (considering building-specific fragility curves for each site according to the design ground motion)

	Max	Min	Median	Mean	CoV*
Annual collapse rate	2.6×10^{-5}	2.5×10^{-9}	5.0×10^{-6}	6.0×10^{-6}	0.89
Probability of collapse in 50 years	1.3×10^{-3}	1.2×10^{-7}	2.5×10^{-4}	3.0×10^{-4}	0.89
*CoV: Coefficient of Variation					

In the current study, the comparison of Table 1 with Table 2 and Table 3 indicates that the value of 10^{-5} for the annual target probability of collapse can be the logical estimate.

The collapse risk distribution was prepared throughout the country to compare the methods used to introduce the building-specific fragility curve. Figure 5 shows the relation between the probability of collapse in 50 years and the design ground motion obtained from the UHGM map (Fig. 1). Figure 5a and Fig. 5c display the collapse probability achieved using the mean fragility curve (mean of 100 values of β and $P_c|gm$ considering the multivariant normal distribution) and considering all 100 values of β and $P_c|gm$ for each site, respectively. On the other hand, all 100 values of β and $P_c|gm$ are assumed to be

similar for all 13500 sites. Figure 5b presents the relation between the risk of collapse and the design PGA related to the fragility curves developed through the introduced function by Crowley, Silva, and Martins (2018), for every 13500 sites (namely building- and site-specific fragility curves). The comparison of Figs. 5a, 5b, and 5c shows that building- and site-specific fragility curves provide a more consistent risk distribution with the uniform hazard map, either for regions with low seismicity or moderate to high seismic areas (Fig. 5b). Taherian and Kalantari (2021) also mentioned that considering the fixed values for $P_c|gm$ would provide the overestimated collapse probability for regions with low seismicity. Figure 5a confirms this outline and shows that considering one fragility curve (fixed values of β and $P_c|gm$) overestimates collapse risk values for low hazard areas. Figure 5c demonstrates that although developing underestimated probability of collapse in areas with high seismicity has been solved, the overestimated values of collapse probability are still observed for some areas with low seismicity. This observation could be due to the 100 fixed values of β and $P_c|gm$ for all 13500 sites. It should be taken into account that the calculation of risk-targeted ground motions using different fragility curves according to design ground motion for each site is computationally very time-consuming. Hence, it is preferred to use the relation between the design ground motion and β and the median value of building capacity to develop a building- and site-specific fragility curve for every desired site. According to this, it is recommended to introduce relationships between the design acceleration and the median (θ) and logarithmic standard deviation (β) of the collapse fragility functions similar to those raised by Crowley, Silva, and Martins (2018) for other typologies and different areas.

As shown in Fig. 5b and Fig. 5c, the results obtained are remarkably similar, confirming the accuracy of the multivariant normal distribution used in this paper

5 Results For Spain

In this section, the risk analysis is performed assuming different fixed values of β and $P_c|gm$ to assess the effect of these parameters on the risk analysis. Then, the risk-targeted maps will be presented across Spain. For this purpose, once the average values of 0.7 and 3×10^{-4} for β and $P_c|gm$ (related to the obtained random sampling using the multivariant normal distribution) are considered, then the building- and site-specific fragility curves are implemented. It should be noted, the considered value of 3×10^{-4} for $P_c|gm$ consistent with the probability of collapse at design ground motion for ordinary structures (not too much low value). This remark was also discussed by Martins et al. (2018). They mentioned a low value of $P_c|gm$ for ordinary structures could be a conservative value. Finally, a risk-targeted map corresponding to different risk level, i.e., yielding (slight damage), is presented.

In the first step, in order to evaluate the effect of two main input parameters, namely the standard deviation β and the probability of collapse for a given design ground motion with a 475-year mean return

period (defining the fragility function) on the risk-targeted ground motion, a series of maps for Spain were generated. For this purpose, four sets of values for β and $P_c|gm$ has been selected, i.e., $\beta \pm \sigma_{\beta}$ and $P_c|gm \pm \sigma_{Pc|gm}$ where σ denotes the standard deviation of the β and $P_c|gm$ with respect to their mean values corresponded to their random normal distribution. Table 4 shows the values assigned for the β and $P_c|gm$. As mention in Sect. 4, we will use the value of 1.0×10^{-5} for the acceptable annual probability of collapse, λ_c, for all the cases. Moreover, the correlation between these parameters is disregarded since we are just looking for the effect of these parameters on the results of risk analysis.

Table 4
Different cases considered for risk analysis in Spain

Number of case	β	$P_c\|gm$	λ_c
Case 1 ($\beta + \sigma_{\beta}$ & $P_c\|gm - \sigma_{Pc\|gm}$)	0.8	1.5×10^{-5}	1.0×10^{-5}
Case 2 ($\beta + \sigma_{\beta}$ & $P_c\|gm + \sigma_{Pc\|gm}$)	0.8	6.2×10^{-3}	1.0×10^{-5}
Case 3 ($\beta - \sigma_{\beta}$ & $P_c\|gm + \sigma_{Pc\|gm}$)	0.6	6.2×10^{-3}	1.0×10^{-5}
Case 4 ($\beta - \sigma_{\beta}$ & $P_c\|gm - \sigma_{Pc\|gm}$)	0.6	1.5×10^{-5}	1.0×10^{-5}

The four maps shown in Fig. 6 represent the risk-targeted ground motions across Spain corresponding to the annual collapse probability of 1.0×10^{-5}. The PGAs were calculated for different combinations of β and $P_c|gm$, according to Table 4.

The comparison between Fig. 6a and Fig. 6d indicates the larger values of β results in the lower risk-targeted ground motion (almost 35% reduction). Moreover, Fig. 6b and Fig. 6c also show a reduction of 19% by increasing the value of β. A general comparison of the two reduction rates demonstrates that the amount of reduction is more remarkable when less probability of collapse for a given ground motion is considered. This could be due to the shape of the fragility curve. Since in the case with a considerable value of β and a small value of the probability of collapse for a given ground motion, the curve will be flatter and will show low values of failure probability even in large earthquakes, which is an unrealistic scenario and in most of the cases leads to low values of risk of collapse with respect to the target value. We have already mentioned that the selection of these values is only to examine the effects of change in these parameters. In addition, this issue outlines the importance of considering the correlation between β and $P_c|gm$. The risk-targeted ground motions in Fig. 6a and Fig. 6b show that for a given value of acceptable collapse probability and standard deviation, the design ground motion level leads to larger values by increasing the value of $P_c|gm$. A comparison between Fig. 6c and Fig. 6d displays the same trend as mentioned before. This trend is expected since, for instance, to achieve a target risk in high seismicity areas despite a high probability of failure, the design ground motion must be increased.

In the next stage of this work, in order to investigate the effects of variation of β and $P_c|gm$ parameters on the risk-targeted ground motions with respect to the UHGM map, a ratio, namely the risk coefficient (CR), is employed. CR is the ratio between PGAs, leading to the target probability of failure and peak ground accelerations with the RP of 475 years (uniform hazard values). As the same as the previous evaluation, the risk-targeted analysis has been performed considering the values of β and $P_c|gm$ mentioned in Table 4. Figure 7 shows the results of this assessment across Spain.

In Fig. 7, a value lower than 1 indicates that the risk-targeted design ground motion is lower than the design ground motion corresponding to the uniform hazard. The distribution of risk coefficients across Spain in Fig. 7a and Fig. 7d shows that the larger β value (i.e., $\beta + \sigma_\beta$) the lower the risk-targeted ground motion design relative to the uniform hazard map (Fig. 1). Figure 7b and Fig. 7c shows the same trend. In addition, the evaluation of these four maps in Fig. 7 illustrates that the modification of design ground motions is more considerable in high seismic regions (e.g., south and southeast of Spain) than in areas with lower seismicity.

In the next step, as mentioned before, once assuming $\beta = 0.7$ and $P_c|gm = 3\times10^{-4}$ and then considering the building- and site-specific fragility curve for every 13500 sites, the risk-targeted ground motion maps across Spain are presented. The target annual collapse probability of 1.0×10^{-5} is considered for all analyses. The results of these analyses are shown in Fig. 8 and Fig. 9. Figure 8a and Fig. 9a display the distribution of risk-targeted design ground motion while Fig. 8b and Fig. 9b show the distribution of risk coefficient for Spain.

As can be seen from Fig. 8a, the risk-targeted ground motion varies between 0.005g and 0.37g with an average value of 0.07g. According to Fig. 9a, the adjusted design ground motion varies between 0.005g and 0.57g, with a mean value of 0.076g. From Fig. 8b and Fig. 9b, we can see that, in most central, western, and northwestern parts of Spain, where they are considered regions with low seismicity, the risk coefficient varies between 0.9 and 1.1. It could be outlined that the risk analysis with the collapse as a risk level does not significantly modify the uniform hazard design PGAs related to the regions with low seismicity. In contrast, as can be seen, most changes occurred in moderate to high seismic areas. Figure 10a and Fig. 10b compare the relation between risk coefficient and uniform hazard design ground motion with a RP of 475 years according to the different types of fragility curves used for risk analysis, i.e., a) mean curve (fixed values of $P_c|gm$, and β) and b) building-site- specific fragility curve using Crowley, Silva, and Martins (2018) fragility functions. From Fig. 9b and Fig. 10b, we can see that to reach a more uniform distribution of collapse risk, we should increase the uniform hazard design ground motion in areas with high seismicity and decrease them in low-to-moderate hazard regions. Moreover, this achieved using the building- and site-specific fragility curves. A comparison of the two figures (i.e., Fig. 10a and Fig. 10b) reveals that employing a unique fragility curve across the country develops underestimated values of risk-targeted design ground motion in areas with moderate to high seismicity,

while there is an opposite trend (i.e., overestimated values of risk-targeted design ground motion) for some low hazard regions. This finding supports evidence from previous observations (e.g., Taherian and Kalantari 2021).

Regarding the low and moderate seismicity areas, as suggested by Douglas et al. (2013) and Silva et al. (2016), it would be more appropriate to use the probability of yielding (slight damage) rather than using the probability of collapse to define the acceptable risk level. For this purpose, to estimate the target annual rate of exceeding slight damage, values of β and probability of exceeding a damaged state (herein yielding) for a given design ground motion ($P_y|gm$) are assumed based on the work by Ulrich et al. (2014), where a set of fragility curves was developed for a regular three-story RC moment frame building designed using EC2 and EC8. Moreover, Martins et al. (2018) found a little variation between the average values of model parameters of fragility curves for yielding damage state corresponded to differently designed buildings. Hence, in this part, we assumed the values mentioned by Ulrich et al. (2014) for β and $P_y|gm$. Using considered values for later parameters and since in Eurocode 8, the damage limitation has been introduced for ground motions with 10% probability of exceedance in 10 years (95-year return period), the same approach than Luco et al. (2007) have done to estimate the acceptable annual probability of yield. The obtained results show that the average annual probability of yielding is $2.5\times10^{-4,}$ and the maximum and minimum values are 2.7×10^{-3} and 1.8×10^{-5}, respectively. Based on the obtained results, we assume a value of 2.5×10^{-4} for the annual target probability of yielding.

Finally, assuming β and $P_y|gm$ values proposed by Ulrich et al. (2014) according to the related design ground motion and target annual yielding probability (λ_y) of 2.5×10^{-4}, the risk-targeted ground motion maps across Spain are developed. The results of these analyses are shown in Fig. 11. Figure 11a and Fig. 11b display the risk coefficient distribution and the corresponding uniform hazard PGA with a mean return period of 95 years for Spain.

Figure 11a and Fig. 11b show that assuming a target annual yielding probability (λ_y) of 2.5×10^{-4} leads to a significant modification of design ground motions across the regions with low or moderate seismicity. In contrast, as expected, Fig. 11a displays an increase of design ground motion in areas with high seismicity to design buildings with the uniform risk of yielding. A comparison of Fig. 11a and Fig. 8b or Fig. 9b also confirms the suggestion by Douglas et al. (2013) and Silva et al. (2016) that slight damage (yielding) be used instead of the collapse risk in low or moderate seismic areas.

In order to investigate the variation in the design ground motion with respect to the uniform hazard PGAs, statistical information related to the risk coefficient in the two assumed risk levels (Table 5) shows that in the collapse performance, the risk coefficient varies between 0.38 and 1.45, while for the yielding risk level, this coefficient changes between 0.063 and 6.2. Moreover, the coefficient of variation for yielding risk level is significantly higher than the one for collapse risk. This indicates that as most of Spain's areas

are regions with low or moderate seismicity, the modification of design ground motion corresponding to the yield risk level is more considerable than for collapse risk level.

Table 5
Statistical results obtained from the risk analysis for Spain (risk coefficient)

Risk level	Max	Min	Median	Mean	CoV*
Collapse	1.45	0.38	1.0	0.95	0.19
Yielding	6.2	0.063	0.52	0.92	1.2
*CoV: Coefficient of Variation					

Table 6 shows the risk coefficient for different acceptable risk levels (i.e., collapse and yielding) corresponding to the cities with the highest seismic hazard, i.e., Valencia, Alicante, Murcia, Almeria, Granada, and Malaga (Fig. 1).

Table 6
Risk coefficient for different acceptable risk levels

	Cities					
Risk level	Valencia	Alicante	Murcia	Almeria	Granada	Malaga
Collapse	1.15	1.18	1.22	1.19	1.16	1.0
Yielding	1.74	2.82	3.64	3.60	3.56	1.64

As shown in Table 6, the results confirm the previous outline in which the modification of design ground motion corresponding to the yield risk level is more considerable than for collapse risk level. Moreover, it can be observed that the PGA design should be increased for almost all cities mentioned above, either for collapsed or yielding risk level. There is only one exception for Malaga, where there is no need for any modification corresponding to the collapse risk level. According to Table 6, Murcia shows the highest increase in design PGA among the cities with high seismic risk. Here, during the Lorca earthquake (11 May 2011, Mw = 5.1) most of the buildings in the Lorca city (Murcia) had reinforced concrete (RC) structures, which, due to their design combined with the severity of the earth tremors, were at serious risk of collapse. In fact, many had to be subsequently demolished and others needed retrofitting (Ruiz-Pinilla et al. 2016). Therefore, this increase in design PGA seems reasonable and necessary.

Clearly, the results of risk-targeted maps would be considerably different by variation of $P_c|gm$, β, and acceptable risk thresholds considered in this study. We also believe that changing the considered typology from RC moment frames into, for instance, masonry ones (the second most familiar buildings in Spain) can also provide completely different results due to the variation in model parameters of corresponding fragility curves.

6 Summary And Conclusions

In this study, risk-targeted maps are developed based on the updated seismic hazard map of Spain. The annual probability was calculated by using the convolution product between seismic hazard and fragility functions. Two risk levels were considered, namely collapse and yielding. Regarding the collapse as a risk level, in order to consider the variability of the relevant parameters for developing the fragility curves, multivariant normal distribution of input parameters (e.g., β and $P_c|gm$) was employed. The framework was based on the information provided by Martins et al. (2018). The effect of variation in the β and $P_c|gm$ parameters on risk analysis results was investigated by considering different values and assumptions, i.e., a fixed value or building- and site-specific fragility models.

Regarding the slight damage risk level, since previous studies (e.g. Martins et al. 2018) indicate there is little variation between relevant input parameters of fragility curves, the values proposed by Ulrich et al. (2014) were considered to perform risk analysis. To calculate the acceptable threshold for the annual probability of exceeding the damage state, the framework similar to Luco et al. (2007) was followed. Furthermore, the risk-targeted ground motion maps were revealed by considering an acceptable risk level probability, and the approach was explained earlier in previous sections. The results highlight these remarks as follow:

- As was expected, structural design based on a ground motion for a given RP results in an annual probability of failure that varies from one area to another. This confirms that the annual probability of collapse depends not only on the ground motion design but also on the shape of the hazard curves in those areas. Of course, the effect of uncertainty on the capacity of structures should not be dismissed.
- The current findings support the relevance of the standard deviation of the fragility curve, β. The larger the β value, the lower the risk-targeted ground motion design relative to the uniform hazard map.
- $P_c|gm$ made a significant difference to annual collapse probability. For a given value of acceptable collapse probability and standard deviation, the design ground motion level leads to larger values by increasing the value of $P_c|gm$.
- This investigation shows that using a fixed value of β and $P_c|gm$ cannot provide an annual probability of collapse in line with the UHGM map. Moreover, it could lead to overestimated or underestimated collapse probability in some low or high hazard areas, respectively.
- Given that these parameters (i.e., acceptable risk probability, standard deviation, and threshold of damage state probability for a given design ground motion) can allocate different values, other risk-targeted maps would be obtained for the considered regions in this study.
- When collapse is assumed as a risk level, the most significant variation in design ground motion is related to high seismicity areas in Spain. In contrast, areas with low or moderate seismicity are slightly affected.

- The modification of design ground motion for low and moderate hazard risk regions corresponding to the yield risk level is more substantial than for collapse risk level.
- The most obvious finding to emerge from this study is that to perform a risk analysis, it is strongly recommended to use fragility models according to the specific typology and commensurate with the design ground motion of that region.

These results show that using different damage states as a risk level is necessary for developing risk-targeted maps to design new buildings. Moreover, the authors also believe that since masonry buildings are the second most common type in Spain, considering different typologies instead of RC moment frames can also provide completely different results due to the variation in model parameters of corresponding fragility curves. Further research needs to establish a clear link between design ground motion in each site and the model parameters of fragility curves similar to works done by Martins et al. (2018), Crowley, Silva, and Martins (2018). The simple relationships between design ground motion and model parameters of fragility curve for a specified typology lead to low computational cost.

Declarations

6 ACKNOWLEDGMENTS

The study has received funding from the European Union's Horizon 2020 research and innovation program under grant agreement No 821046, the Ministerio de Economía, Industria y Competitividad through research project CGL2016-77688-R, with the collaboration and funding provided by Elche and Alicante municipalities.

References

ASCE (2016) ASCE STANDARD Loads for Buildings. Minimum Design Loads for Buildings and Other Structures (ASCE 7-10)

Benito MB, Gaspar-Escribano JM, Rivas-Medina A, Ruiz BS, Cabañas L, Martinez JM (2013) Actualización de Mapas de Peligrosidad Sísmica de España 2012. DOI: 10.7419/162.05.2017

Crowley H, Silva V, Martins L (2018) Seismic Design Code Calibration Based on Individual and Societal Risk. 16th European Conference on Earthquake Engineering June: 173–222

Dolšek M (2009) Incremental Dynamic Analysis with Consideration of Modeling Uncertainties. Earthquake Engineering & Structural Dynamics 38 (6): 805–25. https://doi.org/https://doi.org/10.1002/eqe.869

Douglas J, Gkimprixis A (2018) Risk Targeting in Seismic Design Codes: The State of the Art, Outstanding Issues and Possible Paths Forward. 2013: 211–223. https://doi.org/10.1007/978-3-319-74724-8_14

Douglas J, Gkimprixis A, and Tubaldi E (2019) Derivation of Risk-Targeted Maps for Italy Based on a Simplified Approach. In Atti Del XVIII Convegno ANIDIS L'ingegneria Sismica in Italia : Ascoli Piceno, 15-19 Settembre 2019. Pisa: Pisa University Press. https://doi.org/10.1400/271009

Douglas J, Ulrich T, Negulescu C (2013) Risk-Targeted Seismic Design Maps for Mainland France. Natural Hazards 65 (3): 1999–2013. https://doi.org/10.1007/s11069-012-0460-6

Eads L, Miranda E, Krawinkler H, Lignos DG (2013) An Efficient Method for Estimating the Collapse Risk of Structures in Seismic Regions. Earthquake Engineering & Structural Dynamics 42 (1): 25–41. https://doi.org/https://doi.org/10.1002/eqe.2191

EN-1998 (2005) Eurocode 8: Design of Structures for Earthquake Resistance. European Committee for Standardization

Fajfar P, Dolšek M (2012) A Practice-Oriented Estimation of the Failure Probability of Building Structures. Earthquake Engineering & Structural Dynamics 41 (3): 531–47. https://doi.org/https://doi.org/10.1002/eqe.1143

Garcia-Mayordome J (2015) Creación de Un Modelo de Zonas Sismogénicas Para El Cálculo Del Mapa de Peligrosidad Sísmica de España. Instituto Geológico y Minero de España. Madrid: IGME

Gkimprixis A, Tubaldi E, Douglas J (2019) Comparison of Methods to Develop Risk-Targeted Seismic Design Maps. Bulletin of Earthquake Engineering 17 (7): 3727–52. https://doi.org/10.1007/s10518-019-00629-w

Gkimprixis A, Tubaldi E, Douglas J (2020) Evaluating Alternative Approaches for the Seismic Design of Structures. Bulletin of Earthquake Engineering 18 (9): 4331–61. https://doi.org/10.1007/s10518-020-00858-4

Iervolino I, Spillatura A, Bazzurro P (2018) Seismic Reliability of Code-Conforming Italian Buildings. Journal of Earthquake Engineering 22 (sup2): 5–27. https://doi.org/10.1080/13632469.2018.1540372

IGME (2015) ZESIS: Base de Datos de Zonas Sismogénicas de La Península Ibérica y Territorios de Influencia Para El Cálculo de La Peligrosidad Sísmica En España

IGN-UPM Working Group (2013) Actualización de Mapas de Peligrosidad Sísmica de España 2012. Edited by Centro Nacional de Información Geográfica. Madrid

Jalayer F, Cornell CA (2003) A Technical Framework for Probability-Based Demand and Capacity Factor Design (DCFD) Seismic Formats. PEER Report 2003/8, 122

Kennedy RP (2011) Performance-Goal Based (Risk Informed) Approach for Establishing the SSE Site Specific Response Spectrum for Future Nuclear Power Plants. Nuclear Engineering and Design 241 (3): 648–56. https://doi.org/10.1016/j.nucengdes.2010.08.001

Liel AB, Haselton CB, Deierlein GG, Baker JW (2009) Incorporating Modeling Uncertainties in the Assessment of Seismic Collapse Risk of Buildings. Structural Safety 31 (2): 197–211. https://doi.org/https://doi.org/10.1016/j.strusafe.2008.06.002

Luco N, Ellingwood BR, Hamburger RO, Hooper JD, Kimball JK, Kircher CA (2007) Risk-Targeted versus Current Seismic Design Maps for the Conterminous United States. Structural Engineering Association of California 2007 Convention Proceedings, 1–13

Martins L, Silva V, Bazzurro P, Marques M (2018) Advances in the Derivation of Fragility Functions for the Development of Risk-Targeted Hazard Maps. Engineering Structures 173 (July): 669–80. https://doi.org/10.1016/j.engstruct.2018.07.028

Mezcua J, Rueda J, Blanco RMG (2004) Reevaluation of Historic Earthquakes in Spain. Seismological Research Letters 75 (1): 75–81. https://doi.org/10.1785/gssrl.75.1.75

Ordaz M, Martinelli F, D'Amico V, Meletti C (2013) CRISIS2008: A Flexible Tool to Perform Probabilistic Seismic Hazard Assessment." Seismological Research Letters 84 (3): 495–504. https://doi.org/10.1785/0220120067

Pavel F, Vacareanu R, Douglas J, Radulian M, Cioflan C, Barbat A (2016) An Updated Probabilistic Seismic Hazard Assessment for Romania and Comparison with the Approach and Outcomes of the SHARE Project. Pure and Applied Geophysics 173 (6): 1881–1905. https://doi.org/10.1007/s00024-015-1223-6

Ruiz-Pinilla JG, Adam JM, Pérez-Cárcel R, et al. (2016) Learning from RC building structures damaged by the earthquake in Lorca, Spain, in 2011. Eng Fail Anal 68:76–86. https://doi.org/10.1016/j.engfailanal.2016.05.013

Silva V, Crowley H, Bazzurro P (2016) Exploring Risk-Targeted Hazard Maps for Europe. Earthquake Spectra 32 (2): 1165–86. https://doi.org/10.1193/112514EQS198M

Spillatura A (2018) From Record Selection to Risk Targeted Spectra for Risk Based Assessment and Design. Dissertation, Scuola Universitaria Superiore IUSS Pavia

Taherian AR, Kalantari A (2019) Risk-Targeted Seismic Design Maps for Iran. Journal of Seismology 23 (6): 1299–1311. https://doi.org/10.1007/s10950-019-09867-6

Taherian AR, Kalantari A (2021) Analysis of the Risk-Targeting Approach to Defining Ground Motion for Seismic Design: A Case Study of Iran. Bulletin of Earthquake Engineering. https://doi.org/10.1007/s10518-020-01023-7

Ulrich T, Negulescu C, Douglas J (2014) Fragility Curves for Risk-Targeted Seismic Design Maps. Bulletin of Earthquake Engineering 12 (4): 1479–91. https://doi.org/10.1007/s10518-013-9572-y

Vacareanu R, Pavel F, Craciun I, Coliba V, Arion C, Aldea A, Neagu C (2018) Risk-Targeted Maps for Romania. Journal of Seismology 22 (2): 407–17. https://doi.org/10.1007/s10950-017-9713-x

Vanzi I, Marano GC, Monti G, Nuti C (2015) A Synthetic Formulation for the Italian Seismic Hazard and Code Implications for the Seismic Risk. Soil Dynamics and Earthquake Engineering 77: 111–22. https://doi.org/10.1016/j.soildyn.2015.05.001

Zaman M, Ghayamghamian MR (2019) Risk-Adjusted Design Basis Earthquake: A Case Study of Tehran Megacity. Bulletin of Earthquake Engineering 17 (7): 3777–99. https://doi.org/10.1007/s10518-019-00625-0

Figures

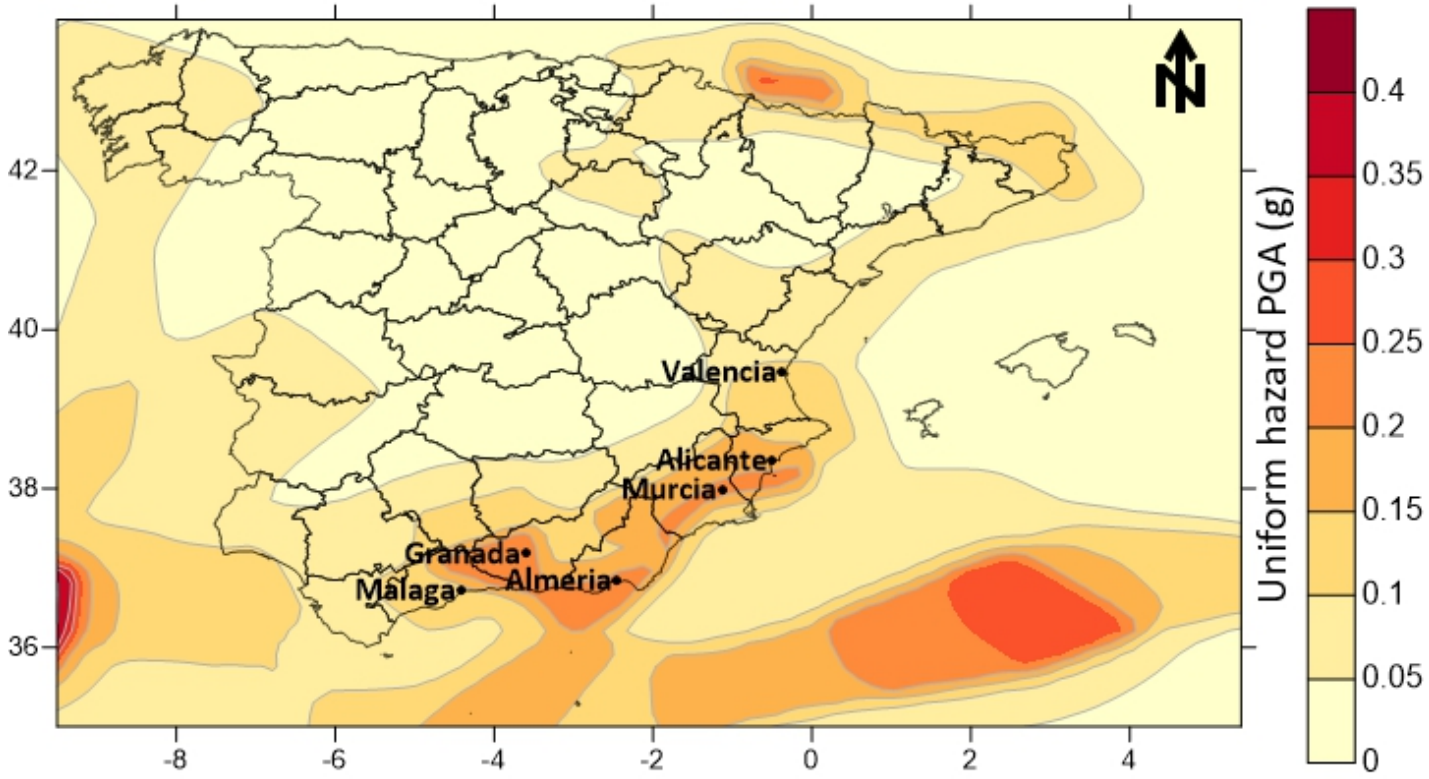

Figure 1

Uniform hazard design ground motion map (UHGM) of Spain (PGA(g) at rock) for 0.1 exceedance probabil-ity in 50 years (Return Period = 475 years) Note: The designations employed and the presentation of the material on this map do not imply the expression of any opinion whatsoever on the part of Research Square concerning the legal status of any country, territory, city or area or of its authorities, or concerning the delimitation of its frontiers or boundaries. This map has been provided by the authors.

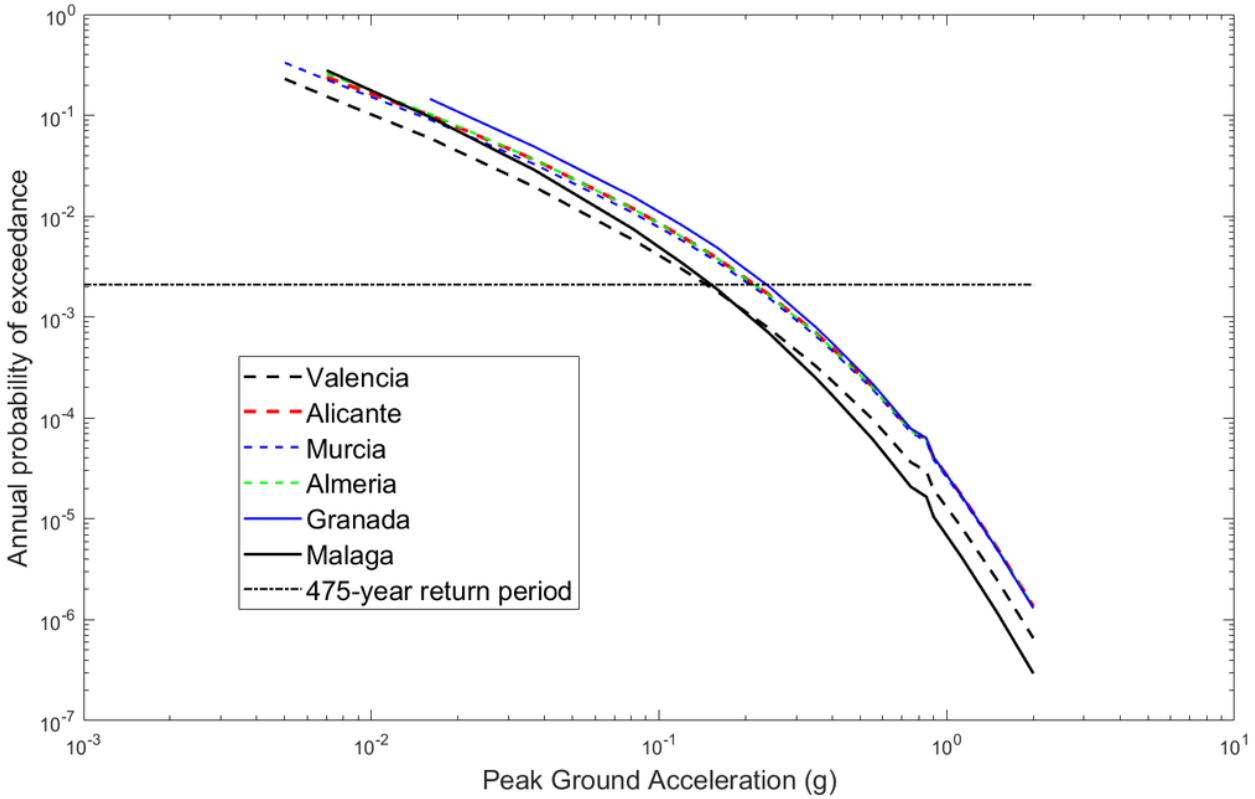

Figure 2

Seismic hazard curves for six selected provinces of Spain

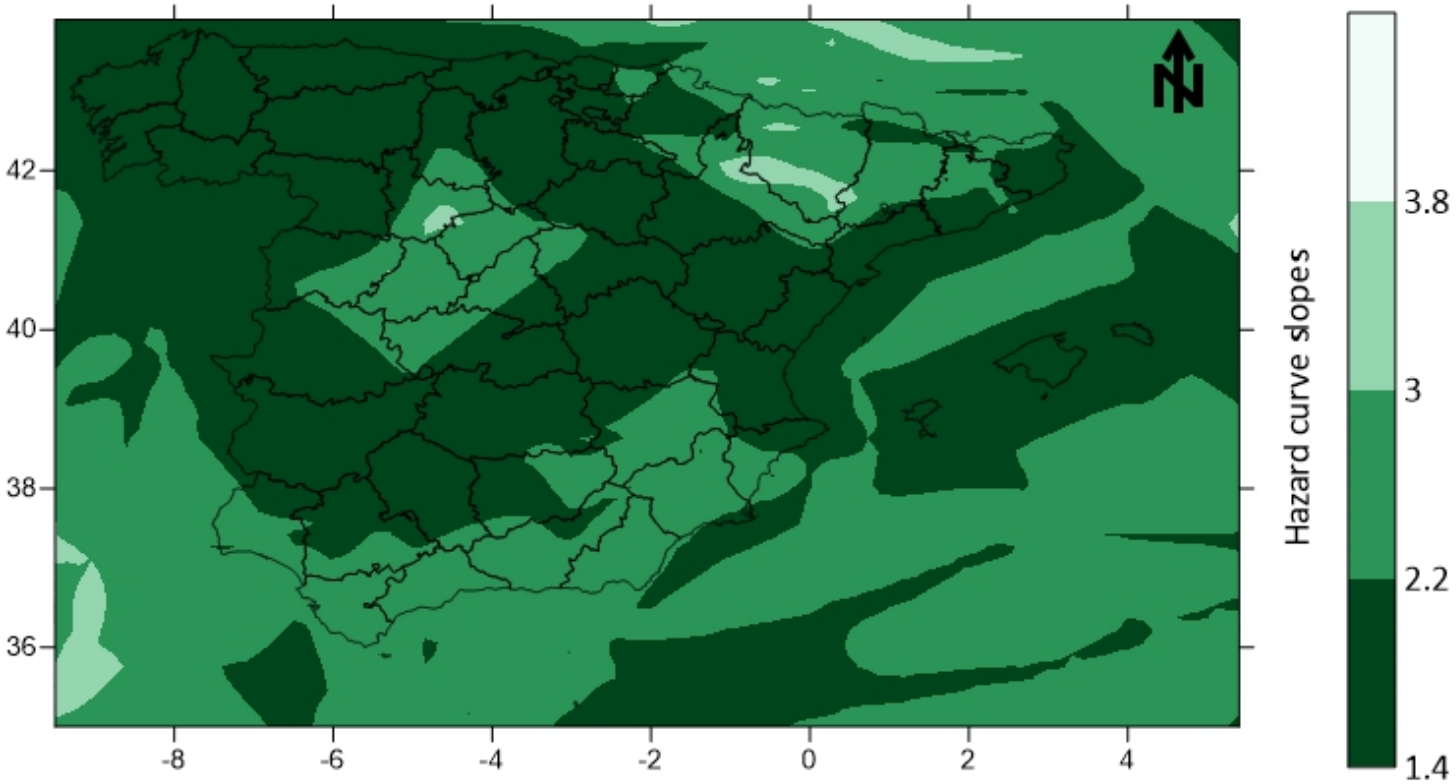

Figure 3

Distribution of local hazard curve slopes Note: The designations employed and the presentation of the material on this map do not imply the expression of any opinion whatsoever on the part of Research Square concerning the legal status of any country, territory, city or area or of its authorities, or concerning the delimitation of its frontiers or boundaries. This map has been provided by the authors.

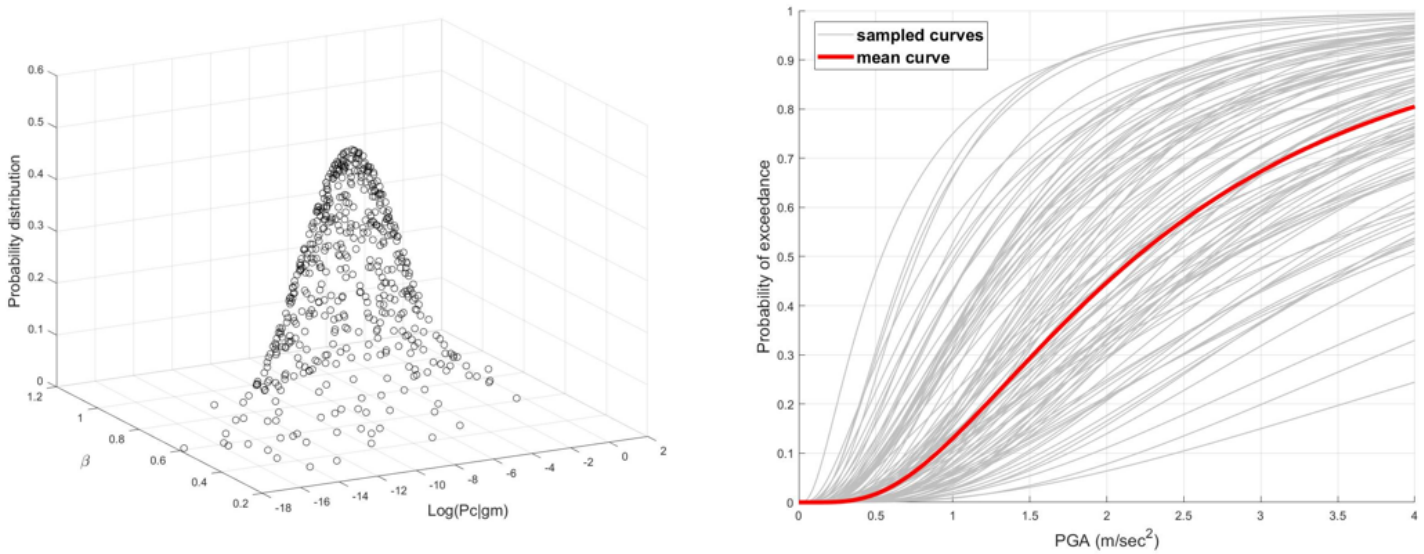

Figure 4

a Multivariant normal distribution for random variables of β and natural logarithmic Pc|gm (correlation coef-ficient = 0.582), b Example of sampled and mean fragility curves using random values estimated through the multivariant PDF at design PGA = 0.2g

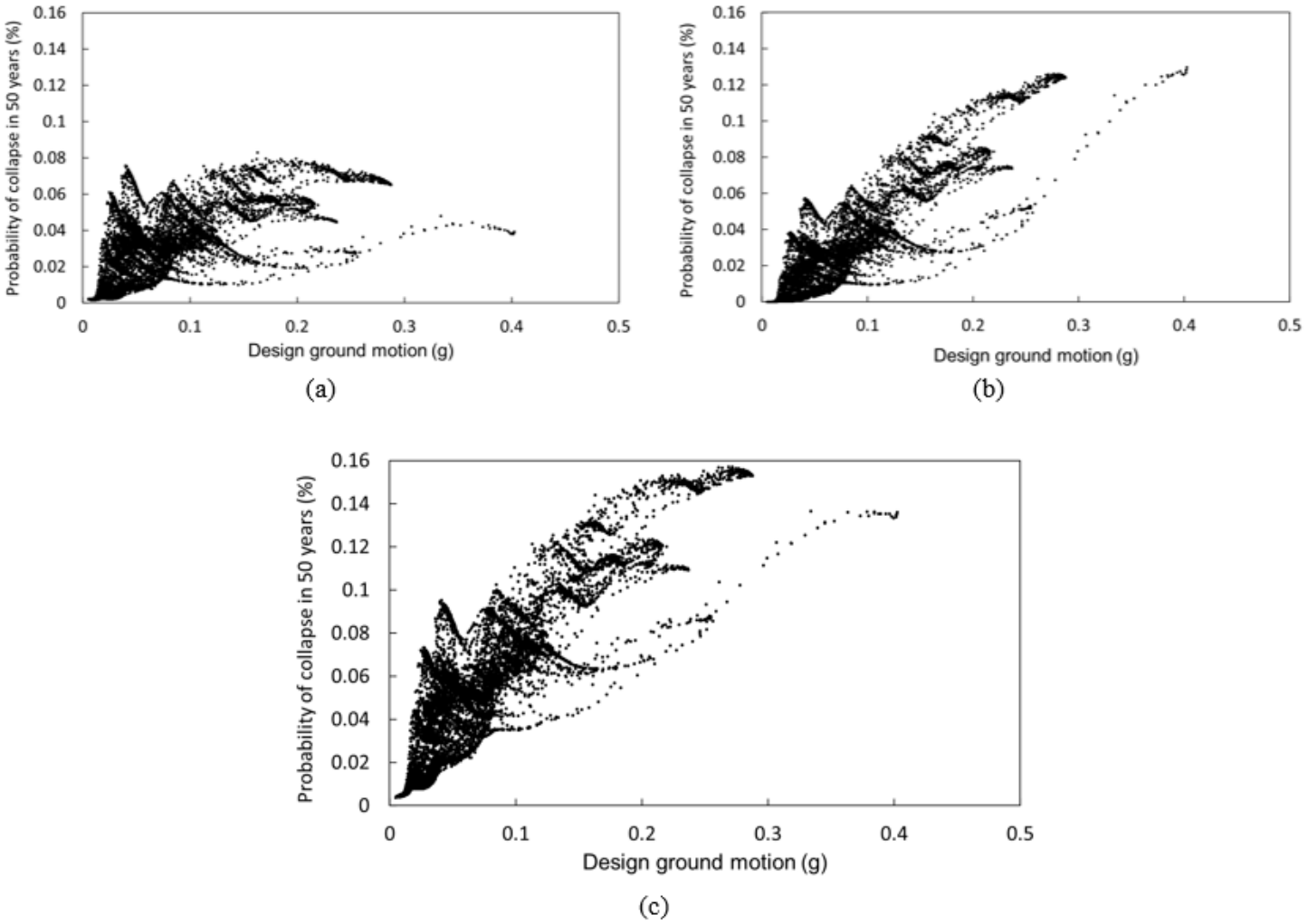

Figure 5

Relation between design ground motion and probability of collapse in 50 years (%) a Fixed value for β and Pc|gm (β = 0.7 and Pc|gm = 3×10-4, b Crowley, Silva, and Martins (2018) fragility curves (building- and site-specific fragility curve), c 100 fixed values of β and Pc|gm for each site obtained from the multivariant normal distribution

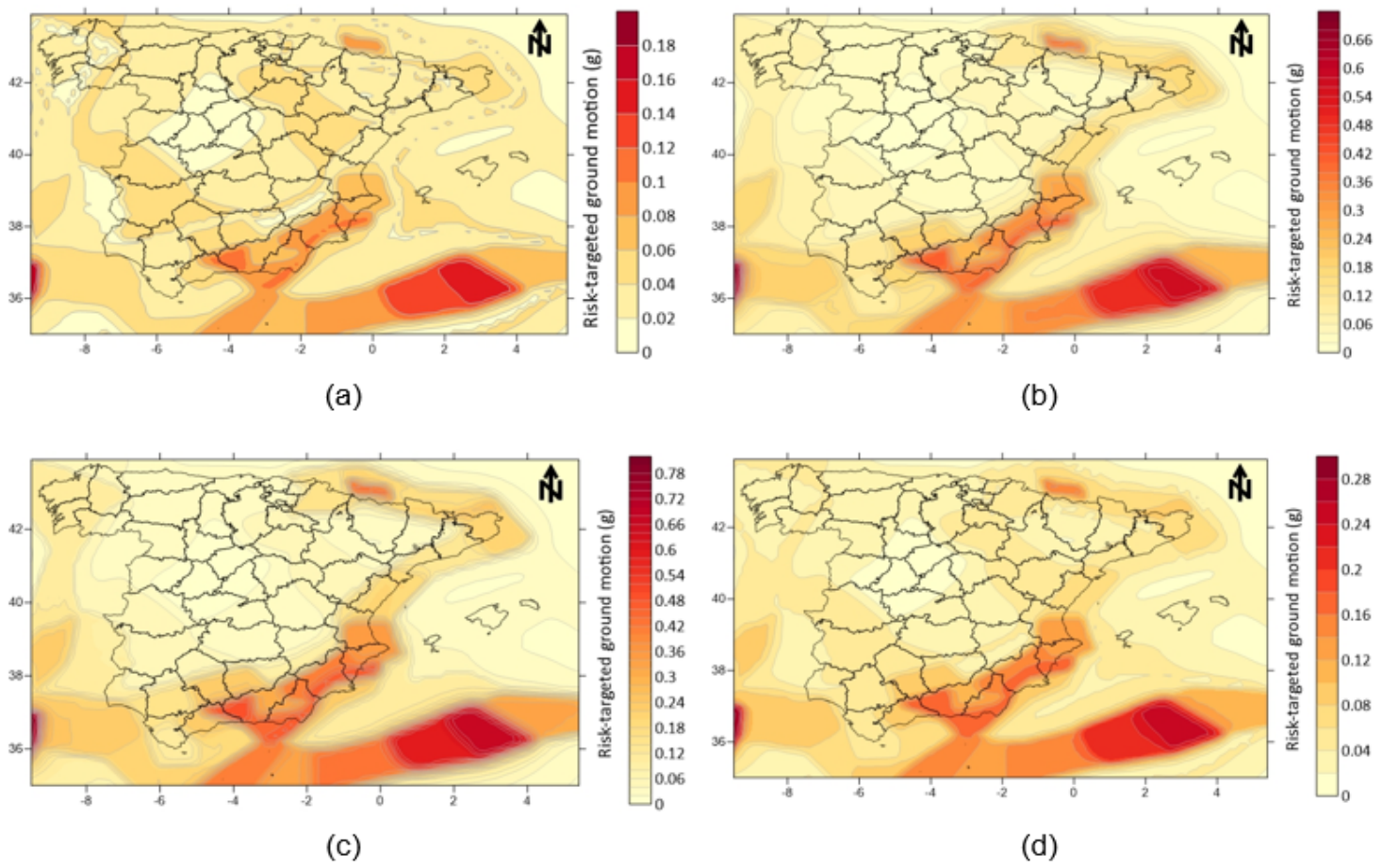

Figure 6

Risk-targeted ground motion maps considering various values of β and Pc|gm (case 1 to case 4) according to Table 4 for Spain a Case 1, b Case 2, c Case 3, d Case 4 Note: The designations employed and the presentation of the material on this map do not imply the expression of any opinion whatsoever on the part of Research Square concerning the legal status of any country, territory, city or area or of its authorities, or concerning the delimitation of its frontiers or boundaries. This map has been provided by the authors.

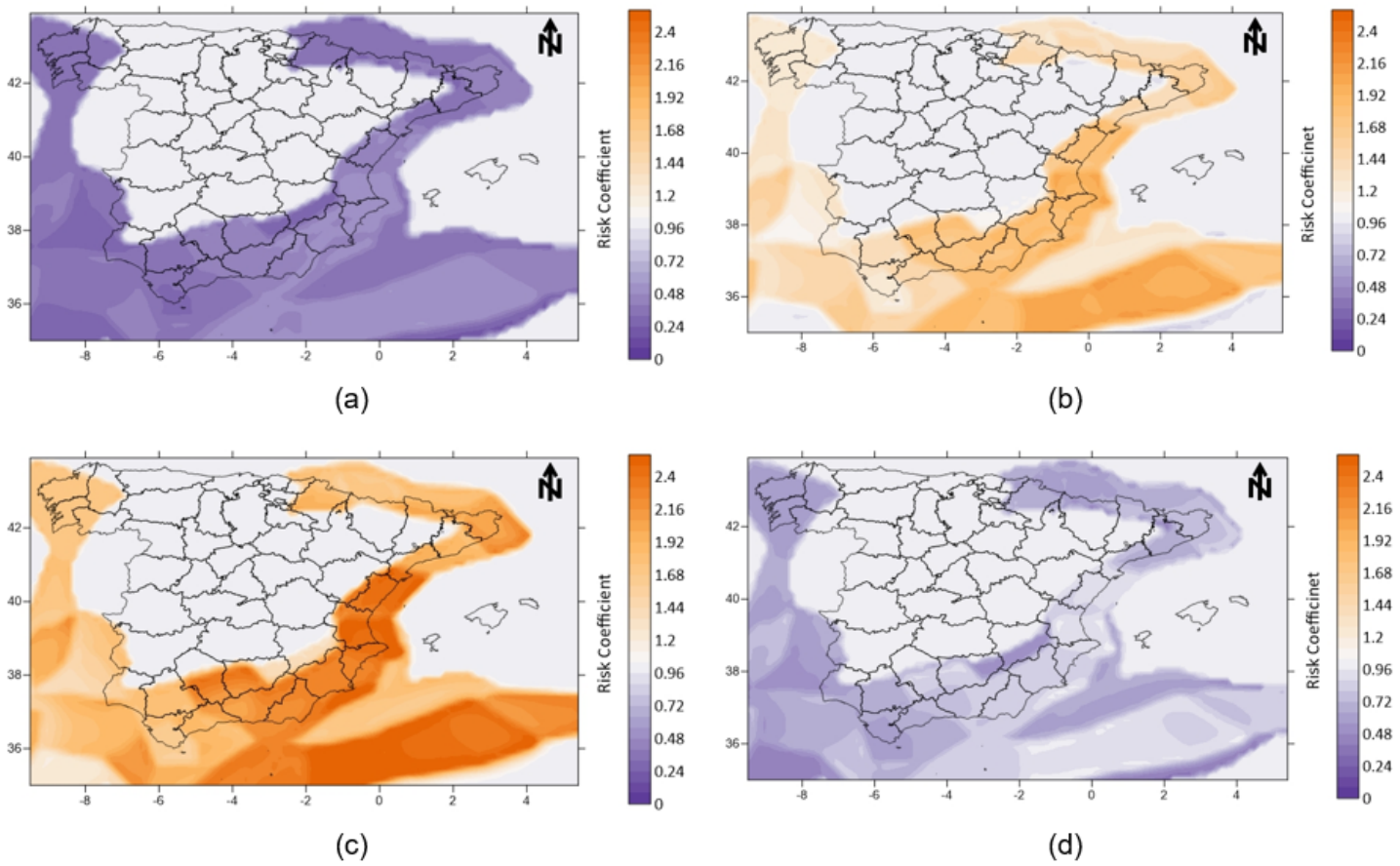

Figure 7

Distribution of risk coefficient considering different values of β and Pc|gm (case 1 to 4) according to Table 4 for Spain a Case 1, b Case 2, c Case 3, d Case 4 Note: The designations employed and the presentation of the material on this map do not imply the expression of any opinion whatsoever on the part of Research Square concerning the legal status of any country, territory, city or area or of its authorities, or concerning the delimitation of its frontiers or boundaries. This map has been provided by the authors.

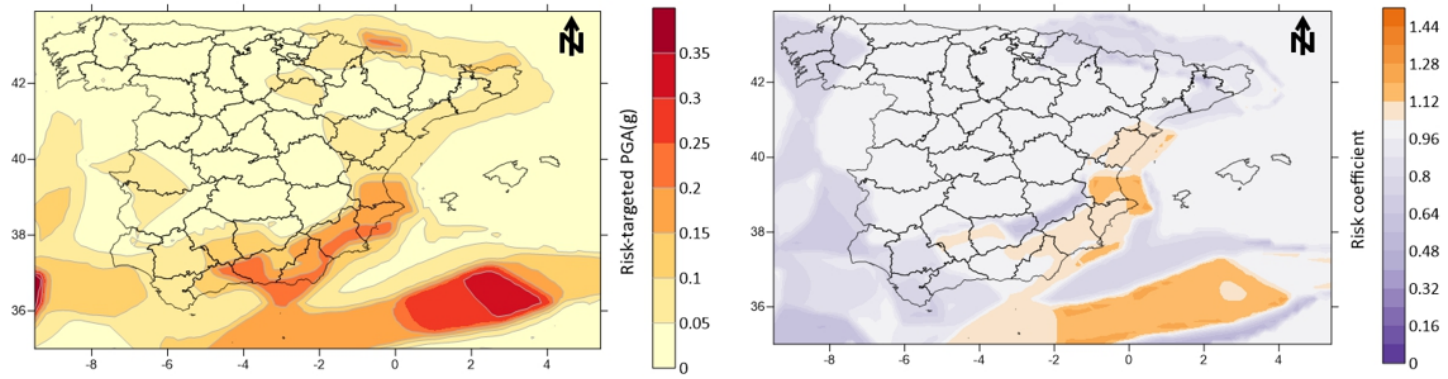

Figure 8

Risk-targeted maps for Spain considering mean curve (fixed values β = 0.7, Pc|gm = 3×10-4, and λc = 1.0×10-5) a Risk-targeted de-sign ground motion, b Risk coefficient Note: The designations employed and the presentation of the material on this map do not imply the expression of any opinion whatsoever on the part of Research Square concerning the legal status of any country, territory, city or area or of its authorities, or concerning the delimitation of its frontiers or boundaries. This map has been provided by the authors.

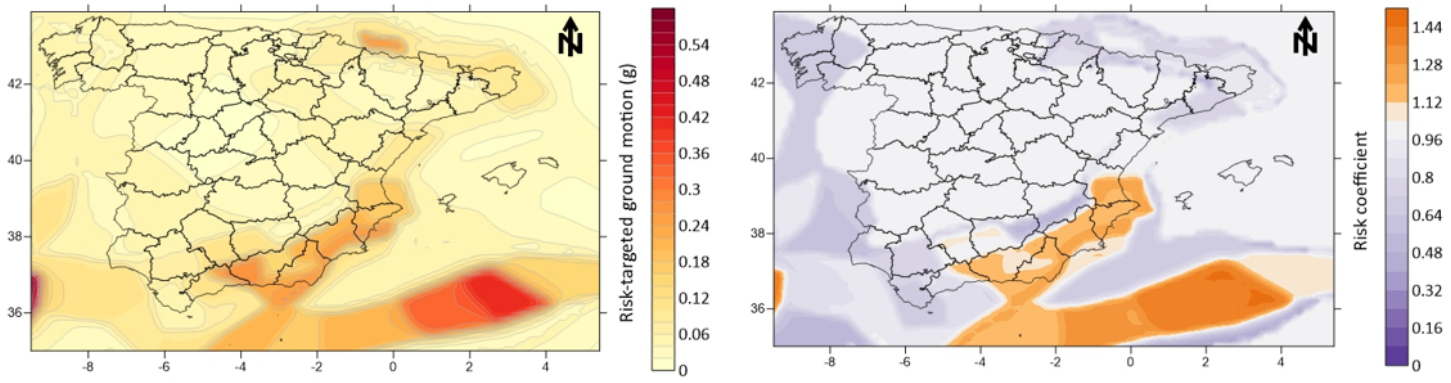

Figure 9

Risk-targeted maps for Spain considering Crowley, Silva, and Martins (2018) fragility functions corresponding to each site a Risk-targeted design ground motion, b Risk coefficient Note: The designations employed and the presentation of the material on this map do not imply the expression of any opinion whatsoever on the part of Research Square concerning the legal status of any country, territory, city or area or of its authorities, or concerning the delimitation of its frontiers or boundaries. This map has been provided by the authors.

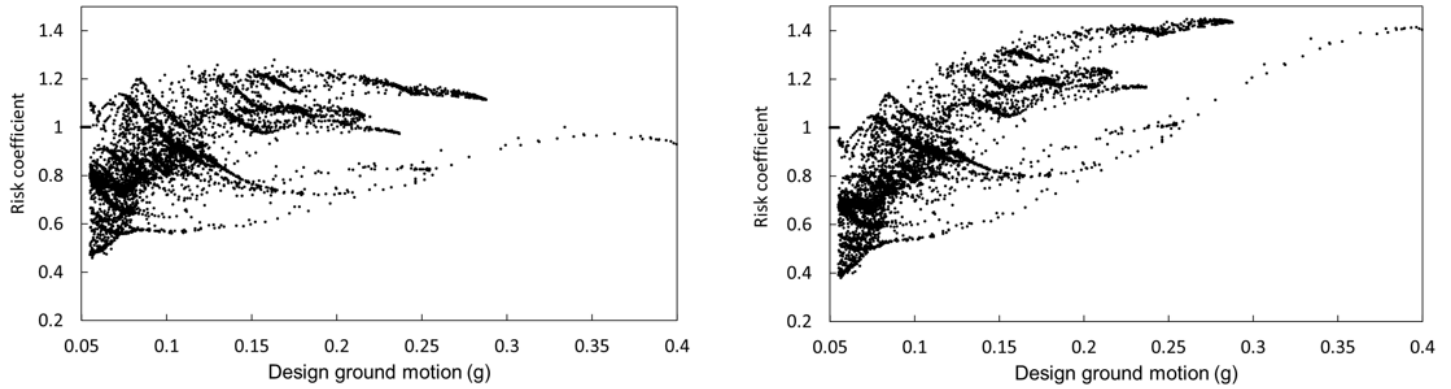

Figure 10

Relation between risk coefficient and uniform hazard design ground motion a Considering mean curve (fixed values of Pc|gm, and beta), b Considering Crowley, Silva, and Martins (2018) fragility curves corresponding to each site

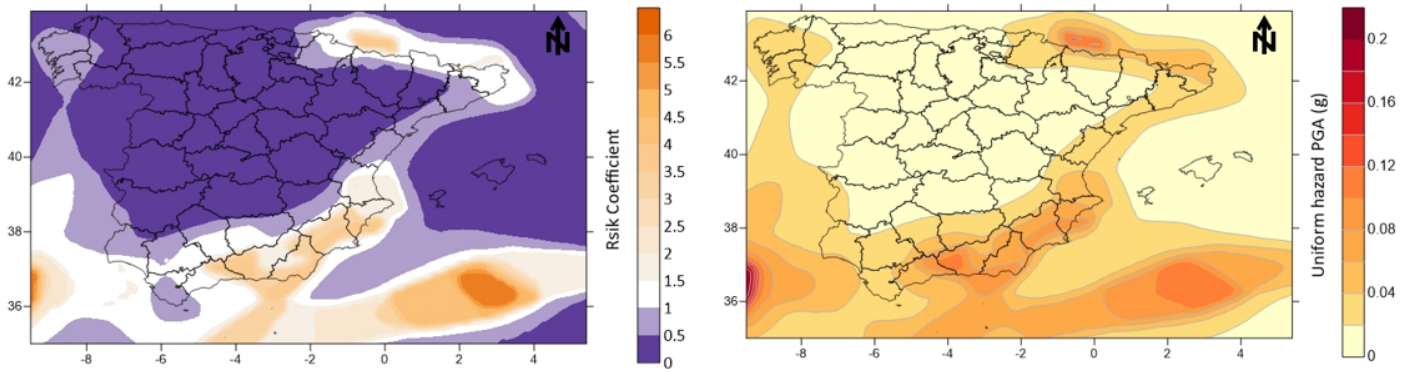

Figure 11

Risk targeted maps for Spain (yielding considered for risk level) a Risk Coefficient distribution (λy = 2.5×10-4), b Uniform hazard map (PGA(g) at rock) with 10% probability of exceedance in 10 years Note: The designations employed and the presentation of the material on this map do not imply the expression of any opinion whatsoever on the part of Research Square concerning the legal status of any country, territory, city or area or of its authorities, or concerning the delimitation of its frontiers or boundaries. This map has been provided by the authors.